Static Mechanical Analysis of Nanobeams Reinforced with Graphene Nanoplatelets Using Modified Couple Stress Theory

Elyakim Aguiar Santana[1], Leonardo Fellipe Prado Leite[1], Fabio Carlos da Rocha[1], Julián B. Castillero[2], Leslie D. P. Fernández[3], Maria do S. M. Sampaio[4]

[1]*Dept. of Civil Engineering, Federal University of Sergipe*
Av. Marcelo Deda Chagas, 49107-230, São Cristóvão - SE, Brazil
elyakim@academico.ufs.br, leolvp@academico.ufs.br, fabiocrocha@academico.ufs.br
[2]*IIMAS Academic Unit at Yucatán, National Autonomous University of Mexico*
Car. Mérida-Tetiz km 4.5, 97357, Ucú - YU, Mexico
julian@mym.iimas.unam.mx
[3]*Dept. of Mathematics and Statistics, Federal University of Pelotas*
Campus Universitário s/n, Prédio 5, 96160-000, Capão do Leão - RS, Brazil
leslie.fernandez@ufpel.edu.br
[4]*Dept. of Civil Engineering, Amazonas State University*
Darcy Vargas Avenue, 69050-020, Manaus-AM, Brazil
msampaio@uea.edu.br

Abstract. Composite materials are fundamental in contemporary engineering, standing out for their ability to combine different raw materials to create new materials with superior properties. Graphene, characterized by its two-dimensional flat carbon monolayer structure with a thickness of 0.34 nm, has gained considerable interest due to its remarkable mechanical, thermal and electrical properties. In particular, graphene derivatives, such as graphene nanoplatelets (GNP) and carbon nanotubes (CNT), have been widely explored as reinforcements in composites. Compared to CNT, GNP offers a more economical alternative and a larger surface area, available in various sizes, from nanometers to micrometers. Studies of micro-nanostructures reinforced with GNP have also evolved, presenting analyses of free vibrations, nonlinear bending and axial instability. This work proposes a variational formulation to model the static mechanical behavior of nanobeams reinforced with graphene nanoplatelets. The modified strain gradient theory of the micromechanical constitutive model, coupled with high-order beam kinematics, is developed to obtain the governing equations and their boundary conditions. The Navier procedure is used to develop an analytical solution for the problem. The results are compared with others in the specialized literature, and the proposed model is proven to be accurate.

Keywords: Graphene Nanoplatelets; Modified Strain Gradient Theory; Nanobeams.

1 Introduction

The static behavior of size-dependent micro/nano beams can be modeled through various approaches, including Molecular Dynamics (MD) methods and higher-order continuum theories. The latter incorporates strain gradients or nonlocal terms, classical material constants, and additional material length scale parameters. While MD methods yield accurate predictions, their high computational cost makes higher-order continuum theories more prominent for modeling size-dependent structural issues. These theories trace their origins to Piola's pioneering work in the 19th century and the contributions of the Cosserat brothers in 1909 (Dell'Isola [1,2], Cosserat [3]). Subsequent developments have categorized these theories into strain gradient theories, microcontinuum theories, and nonlocal elasticity (Thai [4]).

Recent technological advancements have introduced functionally graded materials (FGM) in micro/nano-electromechanical systems (MEMS/NEMS), as discussed by Witvrouw & Mehta [5], Mohammadi-Alasti [6] and Wei [7]. Graphene, a two-dimensional carbon monolayer, has garnered significant interest due to its exceptional mechanical, thermal, and electrical properties. Derivatives like graphene nanoplatelets (GNP) and carbon nanotubes (CNT) are widely studied as composite reinforcements, with GNP being a more economical alternative with a larger surface area (Yee [8]) . Sahmani advanced the studies by analyzing micro-nanobeams, as well as micro-nanoplates (GNPRC), focusing on the vibrational response and nonlinear bending of micro and nanobeams [9,10], as well as the axial instability of micro and nanoplates[11].

Therefore, this work advances the study of GNP by proposing a variational formulation to model the static mechanical behavior of micro-nanobeams GNPRC. A micromechanical constitutive model, based on the Modified Strain Gradient Theory and higher-order beam kinematics, is developed to derive the governing equations. The Navier procedure is employed to obtain an analytical solution to the problem.

2 Mathematical Development

2.1 Definitions

Fig. 1 shows a simply supported beam reinforced with size-dependent graphene nanoplatelets (GNPRC), with the x and z axes representing the abscissa and ordinate axes, respectively. The beam has a height h and a length L, and is subjected to a load $q(x)$ and a dispersion pattern of U-GNPRC.

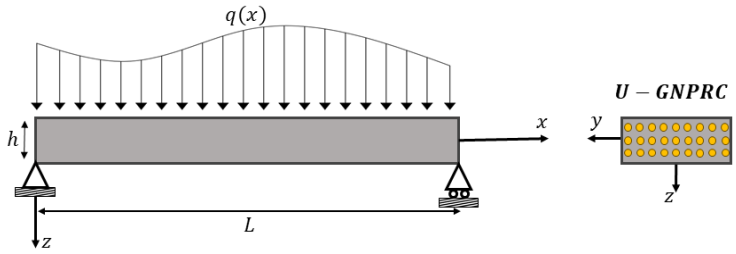

Figure 1. Beam with distributed loading and dispersion pattern uniform.

The volume fraction, V_{GNP}, corresponding to the GNP distribution patterns U-GNPRC can be expressed by eq. (1), as per [12]:

$$U-GNPRC:\ V_{GNP}=\frac{W_{GNP}}{W_{GNP}+\left(\rho_{GNP}/\rho_m\right)\left(1-W_{GNP}\right)}, \tag{1}$$

where W_{GNP} is the weight fraction GNP, ρ_{GNP} and ρ_m are the mass densities of the GNP and the matrix, respectively.

According to the modified Halpin-Tsai micromechanical model (Yang [13] and Affdl & Kardos [14]), the effective Young's modulus, E_c, and effective Poisson's ratio, ν_c, of nanocomposites with randomly oriented nano-reinforcements can be approximated by eq. (2):

$$\begin{aligned} &E_c=\left(\frac{3}{8}\frac{1+\lambda_L\eta_L V_{GNP}}{1-\eta_L V_{GNP}^{(k)}}+\frac{5}{8}\frac{1+\lambda_T\eta_T V_{GNP}}{1-\eta_T V_{GNP}^{(k)}}\right)E_m,\ \nu_c=\nu_{GNP}V_{GNP}+\nu_m\left(1-V_{GNP}\right),\\ &\lambda_L=\frac{2L_{GNP}}{h_{GNP}},\ \eta_L=\frac{E_{GNP}/E_m-1}{E_{GNP}/E_m+\lambda_L},\ \lambda_T=\frac{2b_{GNP}}{h_{GNP}},\ \eta_T=\frac{E_{GNP}/E_m-1}{E_{GNP}/E_m+\lambda_T}, \end{aligned} \tag{2}$$

where λ_L and λ_T are dimensionless parameters dependent on the geometry of the nano-reinforcement. Similarly, η_L and η_T depend on Young's moduli of the matrix, nano-reinforcement, and dimensionless

parameters.

2.2 Kinematics

The present formulation assumes that the material is linearly elastic. Based on various beam theories, the displacement field is expressed by eq. (3):

$$u_x\left(x,z\right)=u_0\left(x\right)-zw_{0,x}+f\left(z\right)\phi_s\left(x\right),\ u_y\left(x,z\right)=0,\ u_z\left(x,z\right)=w_0\left(x\right), \tag{3}$$

where u_0 is the axial displacement along the centroidal axis, w_0 the transverse displacement along the centroidal axis, $f\left(z\right)$ is a function that represents the distribution of high-order shear stress and strain along the depth of the beam (wich, in this work, uses the a function of Soldatos [15]), $\phi_s\left(x\right)=w_{0,x}\left(x\right)+\psi\left(x\right)$ is the angle due to shear. The subscripts following the comma represent the derivatives of the function.

The linear elastic strain field can be expressed using eq. (4) and (5).

$$\varepsilon_{ij}=\frac{1}{2}\left(u_{i,j}+u_{j,i}\right),\ \gamma_i=\varepsilon_{mm,i},\ \eta^{(1)}_{ijk}=\eta^s_{ijk}-\frac{1}{5}\left(\delta_{ij}\eta^s_{mmk}+\delta_{jk}\eta^s_{mmi}+\delta_{ki}\eta^s_{mmj}\right), \tag{4}$$

$$\eta^s_{ijk}=\frac{1}{3}\left(u_{i,jk}+u_{j,ki}+u_{k,ij}\right),\ \chi^s_{ij}=\frac{1}{2}\left(e_{ipq}\varepsilon_{qj,p}+e_{jpq}\varepsilon_{qi,p}\right), \tag{5}$$

where ε_{ij} is the strain tensor, γ_i is the dilation gradient tensor, $\eta^{(1)}_{ijk}$ is the second-order displacement gradient tensor, η^s_{ijk} is the symmetric part of the second-order displacement gradient tensor, and χ^s_{ij} is the symmetric rotation gradient tensor. The constitutive relations for a linear elastic material are expressed in eq. (6).

$$\sigma_{ij}=\kappa\delta_{ij}\varepsilon_{mm}+2\mu\varepsilon'_{ij},\ p_i=2\mu l_0^2\gamma_i,\ \tau^{(1)}_{ijk}=2\mu l_1^2\eta^{(1)}_{ijk},\ m^s_{ij}=2\mu l_2^2\chi^s_{ij}, \tag{6}$$

where σ_{ij} is the classical stress tensor, and p_i, τ_{ijk}, and m^s_{ij} are the higher-order stress tensors. κ and μ are the bulk and shear moduli, respectively. l_0, l_1, and l_2 are the material characteristic lengths associated with the dilation gradient, the second-order displacement gradient, and the symmetric rotation gradient, respectively. The indexes $i,j,k=\left(1,2,3\right)=\left(x,y,z\right)$, as well as the index $m=\left(1,2,3\right)$ indicate summation when repeated, δ_{ij} is Kronecker delta and e_{ijk} permutation symbol.

2.3 Governing equations

The principle of minimum total potential energy Reddy [16] , is used to derive the governing equations, and eq. (14) describes its general expression:

$$\delta\Pi\equiv\delta\left(U+W_{ext}\right)=0, \tag{7}$$

where U is the strain energy and W_{ext} is the external energy, described in eq. (15):

$$U=\frac{1}{2}\int_\Omega(\sigma_{ij}\varepsilon_{ij}+p_i\gamma_i+\tau^{(1)}_{ijk}\eta^{(1)}_{ijk}+m^s_{ij}\chi^s_{ij})dV;\ W_{ext}=-\int_0^L u_z\left(x,z\right)q\left(x\right)dx, \tag{8}$$

To find the strain fields, substitute eq. (3) into eq. (4) and (5), and then use these results in the constitutive relations given by eq. (6). To apply the first variation of a functional, use the strain fields and the constitutive relations, and then substitute eq. (8) into eq. (7).

We obtain the Euler equations in eq. (9) by applying the necessary condition for minimum total potential energy principle ($\delta\Pi=0$) and using the fundamental lemma of the calculus of variations:

$$
\begin{aligned}
\delta u_0 :\ & \Big[A_7 u_{0,xx}(x) - A_8 u_{0,xxxx}(x) + \frac{1}{2}(-A_9 + A_{16}) w_{0,xxx}(x) \\
& -\frac{1}{2} A_{17} w_{0,xxxxx}(x) + \frac{1}{2}(A_{12} - A_9)\psi_{,xx}(x) - \frac{1}{2} A_{14}\psi_{,xxxx}(x)\Big] = 0, \\
\delta w_0 :\ & \Big[\frac{1}{2}(-A_{16} + A_9) u_{0,xxx}(x) + \frac{1}{2} A_{17} u_{0,xxxxx}(x) \\
& + A_4 w_{0,xx}(x) + (A_{11} - A_5) w_{0,xxxx}(x) + A_6 w_{0,xxxxxx}(x) \\
& + A_1\psi_{,x}(x) + \frac{1}{2}(A_{10} + A_{11} - A_{13})\psi_{,xxx}(x) + \frac{1}{2} A_{15}\psi_{,xxxxx}(x) + q(x)\Big] = 0, \\
\delta\psi :\ & \big[(-A_{12} + A_9) u_{0,xx}(x) + A_{14} u_{0,xxxx}(x) \\
& + 2A_1 w_{0,x}(x) + (A_{10} + A_{11} - A_{13}) w_{0,xxx}(x) + A_{15} w_{0,xxxxx}(x) \\
& + 2A_1\psi(x) + 2(A_{10} - A_2)\psi_{,xx}(x) + 2A_3\psi_{,xxxx}(x)\big] = 0,
\end{aligned}
\tag{9}
$$

where the constants A_i are presented in eq. (10):

$$
\begin{aligned}
A_1 &= b\int_{-\frac{h}{2}}^{\frac{h}{2}}\left(k_s\mu\left(f_{,z}(z)\right)^2 + \frac{1}{60}\left(32l_1^2 + 15l_2^2\right)\mu\left(f_{,zz}(z)\right)^2\right)dz, \\
A_2 &= b\int_{-\frac{h}{2}}^{\frac{h}{2}}\left(\left(k + \frac{4\mu}{3}\right)f(z)^2 + \frac{1}{60}\left(120l_0^2 + 128l_1^2 + 15l_2^2\right)\mu\left(f_{,z}(z)\right)^2\right)dz, \\
A_3 &= b\int_{-\frac{h}{2}}^{\frac{h}{2}}\left(\frac{2}{5}\left(5l_0^2 + 2l_1^2\right)\mu f(z)^2\right)dz,\ A_4 = b\int_{-\frac{h}{2}}^{\frac{h}{2}}\left(k_s\mu\left(f_{,z}(z)\right)^2 + \frac{1}{60}\left(32l_1^2 + 15l_2^2\right)\mu\left(f_{,zz}(z)\right)^2\right)dz, \\
A_5 &= b\int_{-\frac{h}{2}}^{\frac{h}{2}}\Bigg(2l_0^2\mu + \frac{8l_1^2\mu}{15} + l_2^2\mu \\
&+ \frac{1}{60}\Big(20(3k + 4\mu)\left(f(z) - z\right)^2 - 4\left(60l_0^2 + 32l_1^2 + 15l_2^2\right)\mu\left(f_{,z}(z)\right) + \left(120l_0^2 + 128l_1^2 + 15l_2^2\right)\mu\left(f_{,z}(z)\right)^2\Big)\Bigg)dz \\
A_6 &= b\int_{-\frac{h}{2}}^{\frac{h}{2}}\left(\frac{2}{5}\left(5l_0^2 + 2l_1^2\right)\mu\left(f(z) - z\right)^2\right)dz,\ A_7 = \int_{-\frac{h}{2}}^{\frac{h}{2}}\left(k + \frac{4\mu}{3}\right)dz, \\
A_8 &= b\int_{-\frac{h}{2}}^{\frac{h}{2}}\left(2l_0^2\mu + \frac{4l_1^2\mu}{5}\right)dz,\ A_9 = \int_{-\frac{h}{2}}^{\frac{h}{2}}\left(-\frac{4}{5}l_1^2\mu\left(f_{,zz}(z)\right)\right)dz, \\
A_{10} &= b\int_{-\frac{h}{2}}^{\frac{h}{2}}\left(-\frac{4}{5}l_1^2\mu f(z)\left(f_{,zz}(z)\right)\right)dz,\ A_{11} = b\int_{-\frac{h}{2}}^{\frac{h}{2}}\left(\frac{4}{5}l_1^2\mu\left(-f(z) + z\right)\left(f_{,zz}(z)\right)\right)dz, \\
A_{12} &= b\int_{-\frac{h}{2}}^{\frac{h}{2}}\left(\frac{2}{3}(3k + 4\mu)f(z)\right)dz, \\
A_{13} &= b\int_{-\frac{h}{2}}^{\frac{h}{2}}\Bigg(\frac{1}{30}\Big(20(3k + 4\mu)f(z)\left(f(z) - z\right) - 2\left(60l_0^2 + 32l_1^2 + 15l_2^2\right)\mu\left(f_{,z}(z)\right) \\
&\quad + \left(120l_0^2 + 128l_1^2 + 15l_2^2\right)\mu\left(f_{,z}(z)\right)^2\Big)\Bigg)dz \\
A_{14} &= b\int_{-\frac{h}{2}}^{\frac{h}{2}}\left(\frac{4}{5}\left(5l_0^2 + 2l_1^2\right)\mu f(z)\right)dz,\ A_{15} = b\int_{-\frac{h}{2}}^{\frac{h}{2}}\left(\frac{4}{5}\left(5l_0^2 + 2l_1^2\right)\mu f(z)\left(f(z) - z\right)\right)dz, \\
A_{16} &= \int_{-\frac{h}{2}}^{\frac{h}{2}}\left(\frac{2}{3}(3k + 4\mu)\left(f(z) - z\right)\right)dz,\ A_{17} = b\int_{-\frac{h}{2}}^{\frac{h}{2}}\left(\frac{4}{5}\mu\left(f(z) - z\right)\left(5l_0^2 + 2l_1^2\right)\right)dz,
\end{aligned}
\tag{10}
$$

2.4 Analytical Solution

The Navier procedure was used to solve the differential equations given by eq. (9). This procedure

approximates the response fields using periodic functions with separated variables. The boundary conditions for a simply supported beam are given by eq. (11), and the solution is assumed by eq. (12):

$$w_0(0) = w_0(L) = 0 \tag{11}$$

$$u_0(x) = \sum_{n=1}^{NT} u_{0_i} \cos\left(\frac{n\pi x}{L}\right), \quad \psi(x) = \sum_{i=1}^{NT} \psi_i \cos\left(\frac{n\pi x}{L}\right), \; w_0(x) = \sum_{n=1}^{NT} w_{0_i} \sin\left(\frac{n\pi x}{L}\right), \tag{12}$$

where NT represents the number of terms in the series. The values of u_{0_i}, ψ_i, and w_{0_i} are obtained by substituting eq. (12) into eq. (9) and solving the resulting algebraic system.

2.5 Results and discussion

Assuming a simply supported beam of height h, length $L = 20h$, width $b = 2h$ and subjected to a concentrated force midspan, $P = 100\mu N$, was adopted. It is considered that the beam is made of GNPRC epoxy with the following properties: $E_m = 1.44$ GPa, $E_{GNP} = 1.01$ TPa, $\rho_m = 1200$ Kg/m³, $\rho_{GNP} = 1062.5$ Kg/m³, $\nu_m = 0.38$, $\nu_{GNP} = 0.186$, $W_{GNP}(\%) = (0{,}1,\ 2,\ 4,\ 6,\ 8 \text{ e } 10)$, and the material length scale parameter $l = 17.6\mu N$ (Lam [17]) . The values of P and h are chosen such that the beam remains elastic throughout (Park [18], Ma [19]). For simplification, we assume that all three material length-scale parameters are the same, i.e. $l_0 = l_1 = l_2 = l$, within the modified high-order strain gradient beam model of the present work. To recover the numerical results from the micro-scale Timoshenko beam model (Wang [20]) , we consider the weight fraction $W_{GNP} = 0\%$, and correction factor $ks = (5+5\nu_m)/(6+5\nu_m)$, as per Kaneko [21] . Fig. 2 shows the results of the modified high-order strain gradient theory beam model and microscale Timoshenko beam models, which illustrate the deflection and rotation for three micro-scale relation, $h = l$, $h = 2l$ and $h = 4l$.

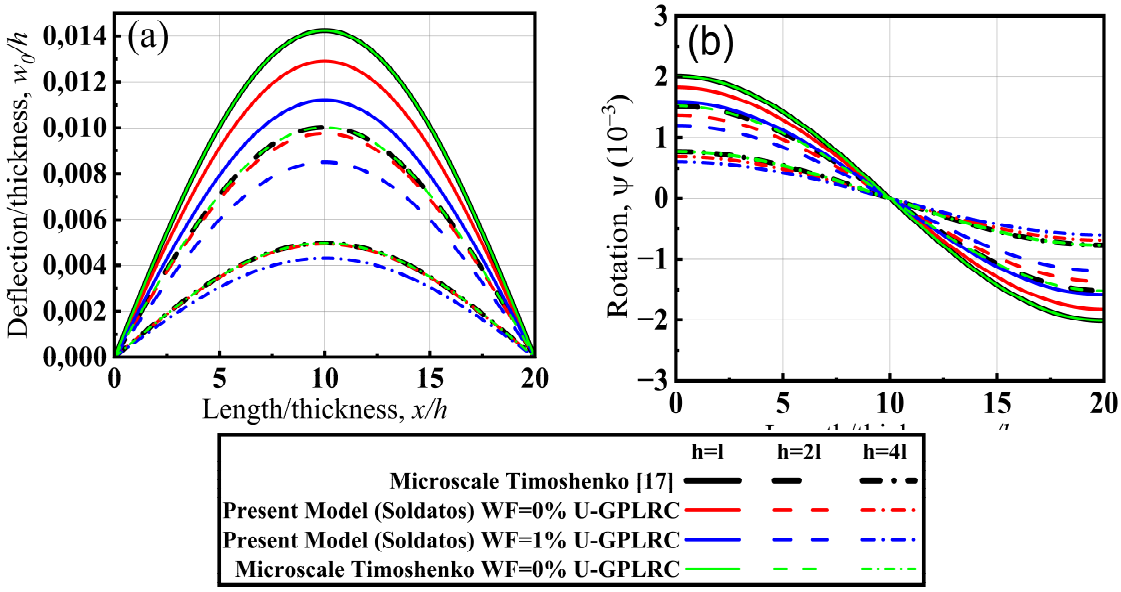

Figure 2- Deflections w_0 and rotations ψ of a beam GNPRC.

It can be observed in Fig. 2(a) that the deflection predicted by the present model, using Soldatos' higher-order beam theory, is smaller than that of the microscale Timoshenko model. This result indicates that the present model exhibits greater bending stiffness because higher-order theories consider the nonlinear variation of shear deformations and size effects, providing a more accurate representation of the response. Similarly, in Fig. 2(b), the Soldatos model showed a smaller rotation compared to the microscale Timoshenko model due to the considerations addressed by higher-order theories. Additionally, the relationship between the beam height and

the length of the nano reinforcement significantly influences the responses; the more significant the beam height relative to the nano-reinforcement, the greater its bending stiffness and, consequently, the smaller the rotation. Furthermore, in Fig. 3(a)-(b), by introducing GNPRCs, there is an increase in bending stiffness and greater resistance to rotation.

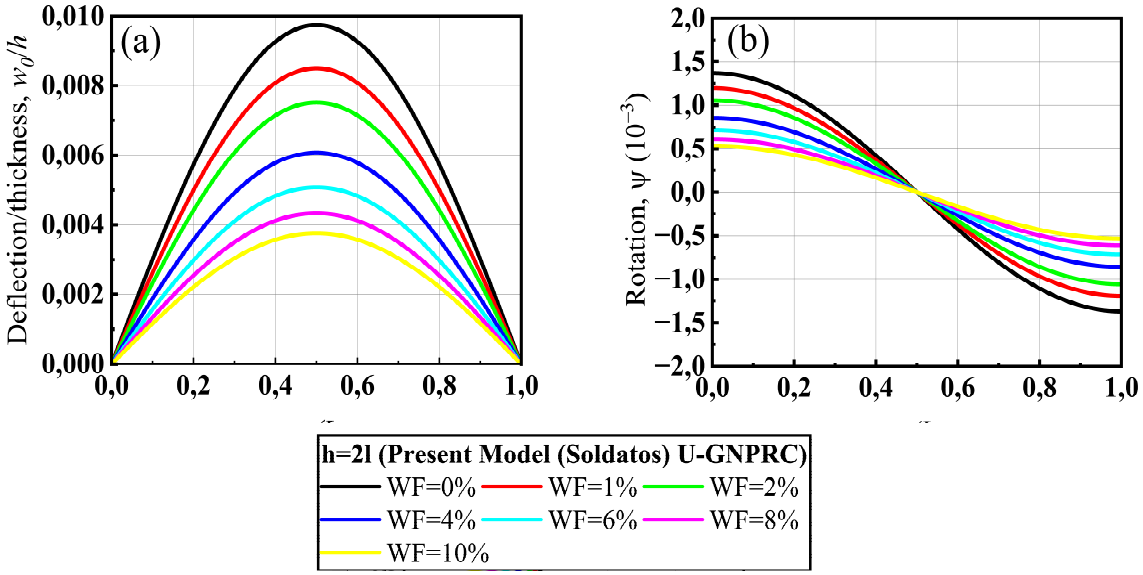

Figure 3- deflection w_0 and rotation ψ of the beam by varying the weight fraction.

3 Conclusions

A modified micromechanical strain gradient constitutive model, coupled with higher-order beam kinematics and reinforced with graphene nanoplatelets, has been developed based on strain gradient elasticity theory and the minimum total potential energy principle. This advanced model can capture deflections and rotations resulting from the size effect associated with material length scale parameters. Additionally, the model allows for the incorporation of nano reinforcements to enhance the mechanical properties of the beam. It is also possible to recover the microscale Timoshenko beam model from this approach concerning reference Lam [17]. The numerical results for deflection and rotation predicted by the new model were compared with those of the microscale Timoshenko beam model under different conditions, such as variations in beam height relative to characteristic length or in the weight fraction of the nano reinforcement. Finally, the proposed model provided consistent results with the higher-order formulation that was presented.

Acknowledgements. E.A.S. and L.F.P.L. thank FAPITEC/SE/FUNTEC and CAPES for their master's scholarships. F.C.R., M.S.M.S., L.D.P.F., and J.B.C. thank CNPq for financial support via Universal Project No 402857/2021-6. Additionally, F.C.R., L.D.P.F., and J.B.C. thank FAPITEC for Universal Project No. 019203.01702/2024-6, and F.C.R. extends thanks to FAPITEC/SE/FUNTEC (Notice No. 02/2024).

Authorship statement. The authors hereby confirm that they are the sole liable persons responsible for the authorship of this work, and that all material that has been herein included as part of the present paper is either the property (and authorship) of the authors, or has the permission of the owners to be included here.

References

[1] Dell'Isola F, Andreaus U, Placidi L. At the origins and in the vanguard of peridynamics, nonlocal and higher-gradient continuum mechanics: An underestimated and still topical contribution of Gabrio Piola. Mathematics and Mechanics of Solids, 2015.
[2] Dell'isola, Francesco et al. Some cases of unrecognized transmission of scientific knowledge: from antiquity to Gabrio Piola's peridynamics and generalized continuum theories. Generalized continua as models for classical and advanced materials, pp. 77-128, 2016.
[3] Cosserat, Eugène Maurice Pierre; COSSERAT, François. Théorie des corps déformables. A. Hermann et fils, 1909.
[4] Thai, Huu-Tai et al. A review of continuum mechanics models for size-dependent analysis of beams and plates. Composite Structures, v. 177, pp. 196-219, 2017.
[5] Witvrouw, Ann; Mehta, Anshu. The use of functionally graded poly-SiGe layers for MEMS applications. In: Materials science forum. Trans Tech Publications Ltd, pp. 255-260, 2005.
[6] Mohammadi-alasti, Behzad et al. On the mechanical behavior of a functionally graded micro-beam subjected to a thermal moment and nonlinear electrostatic pressure. Composite Structures, v. 93, n. 6, pp. 1516-1525, 2011.
[7] Wei, Q. F.; Wang, X. Q.; Gao, W. D. AFM and ESEM characterisation of functionally nanostructured fibres. Applied surface science, v. 236, n. 1-4, pp. 456-460, 2004.
[9] Sahmani, S.; Aghdam, M. M. Nonlocal strain gradient beam model for nonlinear vibration of prebuckled and postbuckled multilayer functionally graded GPLRC nanobeams. Composite Structures, v. 179, p. 77-88, 2017.
[10] Sahmani, Saeid; Aghdam, Mohammad Mohammadi; Rabczuk, Timon. Nonlinear bending of functionally graded porous micro/nano-beams reinforced with graphene platelets based upon nonlocal strain gradient theory. Composite Structures, v. 186, p. 68-78, 2018.
[11] Sahmani, Saeid; Aghdam, Mohammad Mohammadi; Rabczuk, Timon. A unified nonlocal strain gradient plate model for nonlinear axial instability of functionally graded porous micro/nano-plates reinforced with graphene platelets. Materials Research Express, v. 5, n. 4, p. 045048, 2018.
[8] Yee, Kelly; Ghayesh, Mergen H. A review on the mechanics of graphene nanoplatelets reinforced structures. International Journal of Engineering Science, v. 186, pp. 103831, 2023.
[12] Liu, Dongying et al. Three-dimensional free vibration and bending analyses of functionally graded graphene nanoplatelets-reinforced nanocomposite annular plates. Composite Structures, v. 229, pp. 111453, 2019.
[13] Yang, Jie; Wu, Helong; Kitipornchai, Sritawat. Buckling and postbuckling of functionally graded multilayer graphene platelet-reinforced composite beams. Composite Structures, v. 161, pp. 111-118, 2017.
[14] Affdl, JC Halpin; Kardos, J. L. The Halpin-Tsai equations: a review. Polymer Engineering & Science, v. 16, n. 5, pp. 344-352, 1976.
[15] K. P. A. Soldatos. transverse shear deformation theory for homogeneous monoclinic plates. Acta Mechanica. vol. 94, pp. 195–220, 1992.
[16] J. N. Reddy Energy principles and variational methods in applied mechanics.Wiley, 2nd Edition, 2002.
[17] Lam, David CC et al. Experiments and theory in strain gradient elasticity. Journal of the Mechanics and Physics of Solids, v. 51, n. 8, pp. 1477-1508, 2003.
[18] Park, S. K.; Gao, X. L. Bernoulli–Euler beam model based on a modified couple stress theory. Journal of Micromechanics and Microengineering, v. 16, n. 11, pp. 2355, 2006..
[19] Ma, H. M.; Gao, X.-L.; Reddy, JN. A microstructure-dependent Timoshenko beam model based on a modified couple stress theory. Journal of the Mechanics and Physics of Solids, v. 56, n. 12, pp. 3379-3391, 2008.
[20] Wang, Binglei; Zhao, Junfeng; Zhou, Shenjie. A micro scale Timoshenko beam model based on strain gradient elasticity theory. European Journal of Mechanics-A/Solids, v. 29, n. 4, pp. 591-599, 2010.
[21] Kaneko, T. On Timoshenko's correction for shear in vibrating beams. Journal of Physics D: Applied Physics, v. 8, n. 16, pp. 1927, 1975.